Indian Journal of Pure & Applied Physics
Vol. 56, December 2018, pp. 989-996

Effect of hydrogen bonding and solvent polarity on the fluorescence quenching and dipole moment of 2-methoxypyridin-3-yl-3-boronic acid

Raveendra Melavanki[a]*, H S Geethanjali[b], J Thipperudrappa[c], Raviraj Kusanur[d], N R Patil[e] & P Bhavya[f]

[a]Department of Physics, M S Ramaiah Institute of Technology, Bangalore 560 054, India

[b]Department of Physics, Bangalore Institute of Technology, Bangalore 560 004, India

[c]Department of Physics, B N M Institute of Technology, Bangalore 560 070, India

[d]Department of Chemistry, Rashtreeya Vidhyalaya College of Engineering, Bangalore 560 059, India

[e]Department of Physics, B V B College of Engineering and Technology, Hubli 580 031, India

[f]Department of Physics, New Horizon College of Engineering, Bengaluru 560 103, India

Received 11 November 2017; accepted 15 May 2018

Two photophysical properties namely, fluorescence quenching and dipole moment (both ground state and excited state) of 2-methoxypyridin-3-yl-3-boronic acid (2MPBA) have been investigated in alcohol environment using steady state fluorescence technique at 300 K. In quenching studies, a rare but not unusual observation; negative Stern-Volmer (S-V) deviation has been noticed. It has been explained using the concept of solute's conformational changes in the ground state due to inter-molecular and intra-molecular hydrogen bonding in alcohol environment. The spectroscopic data has been processed using Lehrer equation and thereby Stern-Volmer constant (K_{SV}) has been evaluated. It has been found to be above 100 for most of the solvents used. The data related to dipole moment has been examined using different solvent polarity functions. Theoretical calculation of dipole moment in the ground state has been done using Gaussian software. The general solute–solvent interactions and hydrogen bond interactions have been found to be operative. An appreciable red shift of about 25 nm in the emission spectra has been identified with the rise in solvent polarity and decrease in molar mass of alcohols. It confirms the $\pi \rightarrow \pi^*$ transition as well as the possibility of intra-molecular charge transfer (ICT) character in the emitting singlet state of 2MPBA.

Keywords: Boronic acid derivative, Fluorescence quenching, Lehrer equation, Solvatochromic shift method, Dipole moment, Alcohols

1 Introduction

Boronic acids and their derivatives are one of the most useful groups of organoboron molecules. Their role can be seen in synthesis, catalysis, analytical chemistry, separation science, biology, medicine, etc. Boronic acid moiety can bind tightly with diol-containing compounds like carbohydrates and hence their derivatives are drawing exclusive attraction in the designing of artificial lectins. Based on the boronic acid-diol interaction, extensive efforts have been focused on the development fluorometric sensors to sense diol-containing compounds[1-5]. In addition, boronic acid and its derivatives have many other potential biological applications. For example, phenylboronic acid is used in the development of electronic sensor in order to detect dopamine; which is a major neurotransmitter playing an important role in the function of central nervous, renal, hormonal and cardiovascular systems[6]. These attractive and novel properties encouraged us to study the fluorescent properties of 2-methoxypyridin-3-yl-3-boronic acid. Fluorescence spectroscopic study reveals vital information regarding the photophysical properties of organic molecules. This paper is intended to report the findings of fluorescence quenching and dipole moment studies of boronic acid derivative in the alcohol environment.

2 Experimental

2.1 Materials

2-methoxypyridin-3-yl-3-boronic acid was synthesized by standard methods[7] and its molecular structure is given in Fig. 1. Spectroscopic grade solvents like methanol, ethanol, isopropanol, heptanol, butanol, octanol and decanol are used without further purification.

*Corresponding author (E-mail: melavanki73@gmail.com)

2.2 Sample preparation

The experimental samples for quenching studies are prepared by dissolving the solute in different alcohols and the concentration adjusted to 1×10^{-4} M. Doubly distilled aniline is employed as quencher. The quencher concentration is varied from 0.00M–0.10M in steps of 0.02M. Initially solvents were degassed by purging with nitrogen gas to avoid the interference of oxygen in the quenching process since oxygen is also a good quencher.

2.3 Spectroscopic measurements

The absorption spectra are measured on a double beam UV-VIS spectrophotometer (Model: Shimadzu UV-1800) and the fluorescence spectra are recorded on fluorescence spectrophotometer (Model: Hitachi F-2700), with perpendicular geometry keeping the operating voltage at 400V and a slit width of 5nm. A typical absorption spectrum and emission spectrum in methanol (in the absence of quencher) are given in Fig. 2 and Fig. 3, respectively. The excitation wavelength is fixed at 281 nm. Emission spectra of 2MPBA in heptanol for different quencher concentration [*Q*] are given in Fig. 4 which illustrates the variation of intensity with respect to [*Q*]. The absorption wavelength of aniline in an alcohol environment[8,9] is about 230nm - 240nm and hence the possibility of inner filter effect is ruled out.

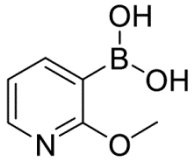

Fig. 1 – Molecular structure of 2-methoxypyridin-3-yl-3-boronic acid (2MPBA).

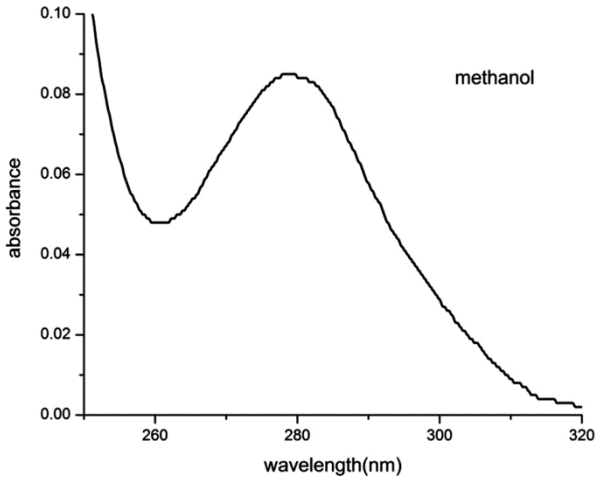

Fig. 2 – Typical absorption spectrum of 2MPBA in methanol.

2.4 Fluorescence life time

Fluorescence life time (τ_0) of the studied compound in different alcohols is measured using a time correlated single photon counting method with nanosecond fluorescence lifetime spectrometer (Model/Make: ChronosBH, USA). The solute is excited with a wavelength of 280 nm. The fluorescence decay profiles are found to be mono exponential in most of the cases. In di or tri exponential cases, the amplitude averaged life time is calculated using the equation[10] $\langle\tau_0\rangle = \sum_i f_i\tau_i$. The quality of the fits is judged from the reduced χ^2 values which is approximately one in all the trials. The fluorescence decay profile in ethanol is given in Fig. 5.

3 Results and Discussion

3.1 Fluorescence quenching

The phenomenon of reducing the fluorescence intensity is known as "quenching" and it is caused due to various reasons like light scattering, inner filter

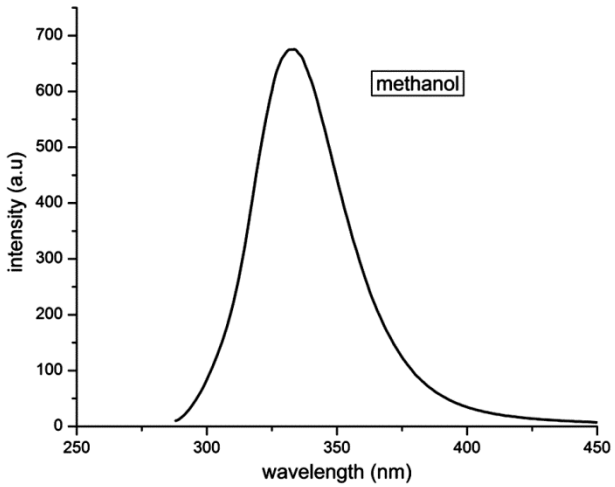

Fig. 3 – Typical emission spectrum of 2MPBA in methanol.

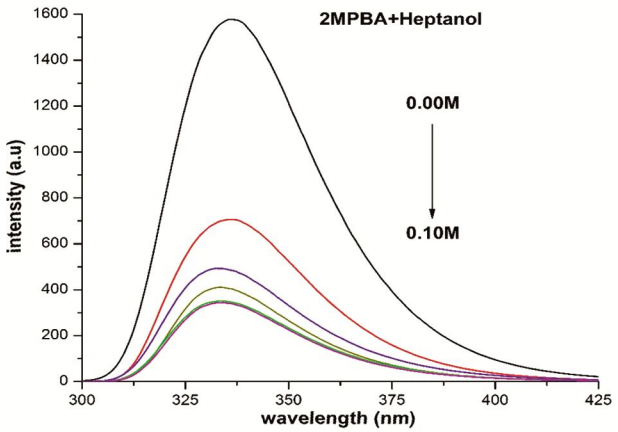

Fig. 4 – Emission spectra of 2MPBA in heptanol with varying quencher concentrations (0.00, 0.02, 0.04, 0.06, 0.08 & 0.10M).

effect (IFE), photo bleaching, self-quenching due to high concentration, etc. Experimentally useful type of quenching is due to collisional interaction between fluorophore and an externally added molecule called 'quencher'. It has been widely studied over the past few decades[11-16] due to its novel applications in various fields. Quenching studies can reveal the localization of fluorophore in the proteins and membranes and their accessibility to the quencher etc[10]. There are two types of quenching namely dynamic and static.

The dynamic quenching process is mainly due to collisions and is governed by the linear Stern–Volmer equation:

$$\frac{I_0}{I} = 1 + K_{SV}[Q] \quad \ldots (1)$$

This is one of the commonly used equations and it relates fluorescent intensities of the molecule in the absence of quencher (I_0) and in the presence of quencher (I) with the quencher concentration [Q]. K_{SV} is Stern-Volmer constant and it mainly describes how the process of quenching is established. For instance, collisional quenching follows linear Stern-Volmer plots and K_{SV} represents the slope. Bimolecular quenching rate parameter (k_q) can calculate using equation:

$$K_{SV} = k_q \tau_0 \quad \ldots (2)$$

where τ_0 is the lifetime of the fluorophore in the absence of quencher.

In static quenching, ground state complex is formed before excitation occurs. These complexed molecules become non fluorescent and hence the number of emitting species reduces. However the fluorescence lifetime is unaffected and Stern-Volmer plot shows a positive deviation. In such cases, the extended Stern–Volmer equation[10] can be used. It is given as:

$$\frac{\left(\frac{I_0}{I}-1\right)}{[Q]} = \left(K_{SV} + K_g\right) + K_{SV}K_g[Q] \quad \ldots (3)$$

here K_g is the ground state association constant and other symbols have their usual meaning.

S-V plots are plotted using I_0 and I values. They are as shown in Fig. 6. These plots are linear in the lower concentration range and deviates towards *x*-axis with the increase in quencher concentration (0.06-0.1M). In the lower quencher concentration range, the linear *S-V* plot implies that the quenching is due to either dynamic (diffusion limited) or static.

Many reasons are quoted in the literature for negative deviation[14,17-20]. One such reason for the negative deviation - presence of two fluorophores with different accessibility to quencher[21]. Quenching data which leads to negative *S-V* plot may be represented Lehrer equation[22,23] given below:

$$I = (1-f)I_0 + \frac{fI_0}{1+K_{SV}[Q]} \quad \ldots (4)$$

where f is the fraction of accessible fluorophores. The linear form of Eq. (4) is:

$$\frac{I_0}{\Delta I} = \frac{1}{f} + \frac{1}{fK_{SV}[Q]} \quad \ldots (5)$$

The linear plots of $I_0/\Delta I$ versus $1/[Q]$ are shown in Fig. 7. The intercept gives $1/f$ and intercept/slope gives *S-V* constant (K_{SV}). The value of f is nearly equal to 1($f \leq 1$) and K_{SV} varies between 73.87 M^{-1} to 798.50 M^{-1}. K_{SV} is also calculated from the linear fit of I_0/I versus lower concentrations [Q]. The values of K_{SV} estimated from both the plots, solvent viscosity (η), quenching rate parameter (k_q) fluorescence life time (τ_0) and diffusion rate constant (k_d) are presented in Table 1.

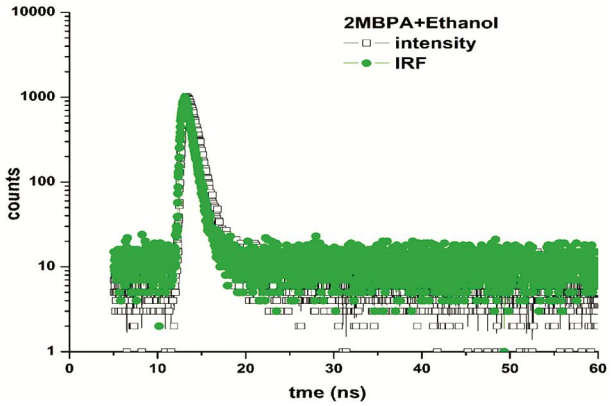

Fig. 5 – Fluorescence decay profile and instrumental response function (IRF) of 2MPBA in ethanol.

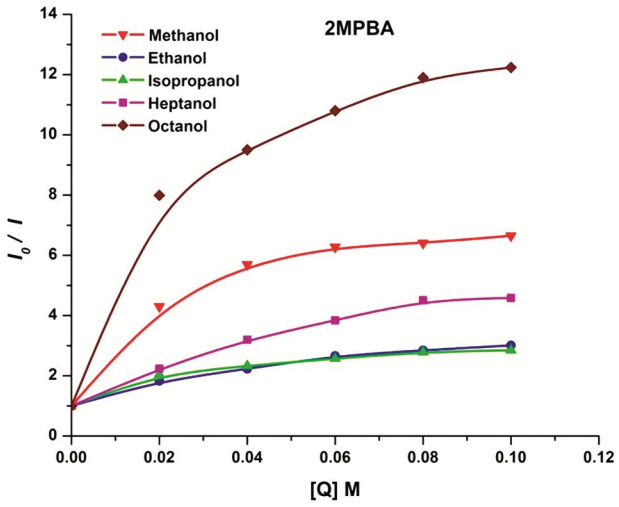

Fig. 6 – *S–V* plots of I_0 / I versus Q exhibiting negative deviation in different solvents for 2MPBA.

A proper interpretation of quenching data and the determination of K_{SV} require identification of the quenching mechanism. From the tabulated values one can make out K_{SV} calculated from the lower concentration part of *S-V* plot is relatively small compare to that obtained from Eq. (5). This entails that the static quenching at the time of excitation (i.e., ground state complex formation) is very weak. Higher value of k_q suggests effective quenching of fluorescence. Henceforth it is analyzed that quenching may take place before the complete formation of a complex in the excited state. Diffusion limited quenching and the role of solvent viscosity (η) is better understood through the calculation of diffusion-limited rate constant k_d using Eq. (6):

$$k_d = 4\pi N' DR \quad \ldots (6)$$

here N' is Avogadro number in per millimole. In diffusion coefficient (cm^2s^{-1}) $D = D_S + D_Q$ and molecular radii (Å) $R = R_S + R_Q$, *S* represents solute and *Q* represents quencher[8,24]. *D* is calculated using Stokes-Einstein equation[25]:

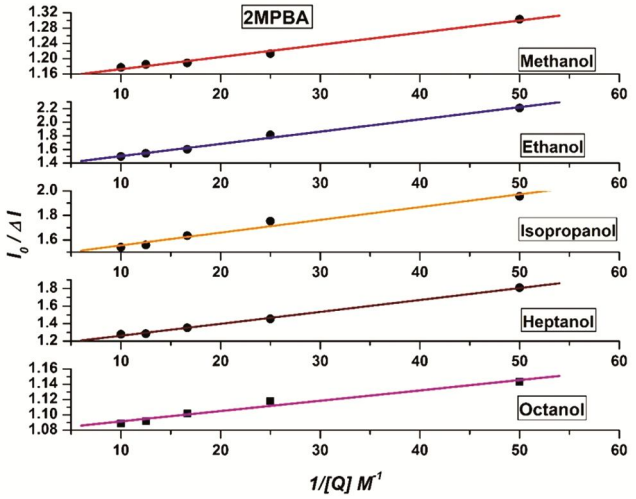

Fig. 7 – Linear plots of $I_0/\Delta I$ versus $1/Q$ in different solvents for 2MPBA.

$$D = \frac{kT}{a\pi\eta R} \quad \ldots (7)$$

here k is Boltzmann constant, T is absolute temperature and '*a*' is Stoke – Einstein number. Its value is 6 for solute and 3 for quencher[8]. The molecular radii (in Å) of the solute and the quencher required for the calculation of k_d are mentioned at the bottom of the Table 1. k_d is inversely proportional to solvent viscosity as it is evident from Eq. (6). These results strongly support the influence of solvent viscosity on quenching mechanism and reactions are to some extent diffusion limited but not totally controlled by material diffusion.

In 2 MPBA, there exists intra-molecular hydrogen bonding between oxygen atom of the methoxy group and hydrogen atom of boronic acid group (Scheme-1). This bonding is highly stable and highly favored because it leads to the formation of a stable six membered chelate as shown in Scheme 1.

The possibility of inter-molecular hydrogen bonding cannot be ruled out in alcoholic solvents. Scheme 2 represents this possibility. Due to the

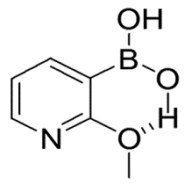

Scheme 1 – Intra-molecular hydrogen bonding.

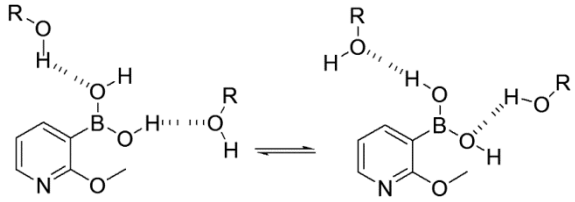

Scheme 2 – Formation of intermolecular hydrogen bonding, where *R* is methyl, ethyl, isopropyl or *n*-butyl groups of different alcohols.

Table 1 – Viscosity (η), fluorescence life time (τ_0), *S-V* constant (K_{SV}), bimolecular quenching rate parameter (k_q) and diffusion rate constant (k_d) of 2MPBA in alcohols.

Solvents	η (cP)	τ_0 (ns)	♣K_{SV} (M^{-1})	$^{\$}K_{SV}$ (M^{-1})	$^{\#}k_q\times10^{-9}$ ($M^{-1}s^{-1}$)	$k_d\times10^{-9}$ ($M^{-1}s^{-1}$)
Methanol	0.544	1.570	117.25	358.74	228.50	18.69
Ethanol	1.200	0.499	30.70	73.87	148.04	8.48
Isopropanol	1.940	0.399	33.23	139.50	349.00	5.24
Heptanol	5.758	4.330	55.00	82.76	19.11	17.94
Octanol	7.360	0.463	212.62	798.50	1724.00	1.38

R (2MPBA) = 3.3613 Å *R* (aniline) = 2.8400 Å

♣ Calculated using lower concentration part of linear *S–V* plots as shown in Fig. 6

$^{\$}$ Calculated using modified Stern – Volmer equation (Lehrer Equation)

$^{\#}$ calculated using $^{\$}K_{SV}$

presence of stable intra-molecular hydrogen bonding and intermolecular hydrogen bonding, the studied solute exists as two different conformers. The existence of two conformers may be the reason for negative deviation in *S-V* plots[15,21].

3.2 Dipole moments

When electromagnetic radiation is incident on a molecule, the electric field associated with the radiation (electric vector) affects the charge cloud around the molecule and hence the dipole moment is disturbed. The change in the dipole moment is influenced by general and specific solvent effects. A study of dipole moments of organic molecules gives vital information which can be used in the design of optical sensors, dye lasers and newer materials for nonlinear optical devices.

3.2.1 Solvent effects on absorption and fluorescence spectra

The solvatochromic data like absorption maxima, emission maxima and Stokes' shift along with E_T^N parameterare listed in Table 2. There is an emission wavelength shift of about 25 nm with the increase in solvent polarity and decrease in molar mass of alcohols. The shift of fluorescence band towards longer wavelength could be due to marked difference between excited state charge distribution and ground state charge distribution. With the increase in solvent polarity, Stokes' shift varies from 3869 cm^{-1} to 6031 $cm^{-1}$with overall change of 2162 cm^{-1}. This indicates that $\pi \rightarrow \pi^*$ transitions are taking place in the excited states.

3.2.2 Estimation of dipole moments

The theoretical ground state dipole moment (μ_g) of 2MPBA is estimated using quantum chemical calculations. The computations are carried out using Gaussian 03 program package on a Pentium-PC with B3LYP/6-31 g* basis set. The ground state dipole moment of this molecule calculated by quantum chemical calculation is found to be 2.59 D.

Different theories are available for the estimation of ground state and excited state dipole moments (μ_g and μ_e) mainly deal with general solvent effects and are based on certain assumptions[10,17-18].

The Bulk solvent polarity parameter ($\Delta f(\varepsilon, n)$) of solvents is determined using Eq. (8):

$$\Delta f(\varepsilon, n) = \left[\frac{\varepsilon-1}{2\varepsilon+1} - \frac{n^2-1}{2n^2+1}\right] \quad \ldots (8)$$

Here ε is dielectric constant and *n* is the refractive index of the solvent. The three independent linear equations used in our study are mentioned below and they have their own limitations[10,17].

Lippert-Mataga's equation relates Stokes' shift $\overline{\Delta\nu}$ with bulk solvent polarity as:

$$\overline{\Delta\nu} = (\bar{\nu}_a - \bar{\nu}_f) = s_1[\Delta f(\varepsilon, n)] + constant \quad \ldots (9)$$

Bakshiev's equation:

$$\overline{\Delta\nu} = s_2[f_1(\varepsilon, n)] + constant \quad \ldots(10)$$

Kawski-Chamma-Viallet's equation:

$$\frac{1}{2}(\bar{\nu}_a + \bar{\nu}_f) = -s_3[f_2(\varepsilon, n)] + constant \quad \ldots(11)$$

where $\bar{\nu}_a$and $\bar{\nu}_f$ are the absorption and emission maxima wavenumbers in cm^{-1}, f_1 and f_2 are the solvent polarity functions given by:

$$f_1(\varepsilon, n) = \frac{2n^2+1}{n^2+2}\left[\frac{\varepsilon-1}{\varepsilon+2} - \frac{n^2-1}{n^2+2}\right] \quad \ldots (12)$$

And

$$f_2(\varepsilon, n) = \frac{2n^2+1}{2(n^2+2)}\left[\frac{\varepsilon-1}{\varepsilon+2} - \frac{n^2-1}{n^2+2}\right] + \frac{3}{2}\left[\frac{n^4-1}{(n^2+2)^2}\right] \quad \ldots (13)$$

Whereas

$$s_1 = \frac{2(\mu_e-\mu_g)^2}{hca^3} \quad \ldots (14)$$

$$s_2 = \frac{2(\mu_e-\mu_g)^2}{hca^3} \quad \ldots (15)$$

And

$$s_3 = \frac{2(\mu_e^2-\mu_g^2)}{hca^3} \quad \ldots (16)$$

Table 2 – Solvatochromic data of 2MPBA in alcohols and Reichardt's solvent polarity parameter (E_T^N).

Solvent	λ_a (nm)	λ_f (nm)	$\Delta f(\varepsilon,n)$	$f_1(\varepsilon,n)$	$f_2(\varepsilon,n)$	E_T^N	$(\bar{\nu}_a - \bar{\nu}_f)$ (cm^{-1})	½$(\bar{\nu}_a + \bar{\nu}_f)$ (cm^{-1})
Methanol	278	334	0.3100	0.8600	0.6500	0.7620	6031	32955
Isopropanol	281.5	331	0.2800	0.7800	0.6500	0.6170	5312	32867
Butanol	280.6	325	0.2638	0.7529	0.6500	0.5860	4868	33203
Octanol	277	321	0.2300	0.6300	0.6000	0.6020	4919	33641
Decanol	276	309	0.2053	0.5564	0.5745	0.5250	3869	34297

Δf = Lippert polarity function; f_1 = Baksheiv polarity function; f_2 = Kawaski – Chammaviallet polarity function.

h is the Planck's constant a is the Onsager cavity radius and c is the speed of light in vacuum. s_1, s_2 and s_3 are slopes of straight lines plotted using Eqs (9), (10) and (11), μ_g and μ_e are the ground state and excited state dipole moments, respectively. Considering the parallel orientation for molecular dipole moments in ground and excited states and assuming absorption and emission take place at the same molecular geometry, Eqs (10) and (11) can be reproduced as below:

$$\mu_g = \frac{s_3 - s_2}{2}\left[\frac{hca^3}{2s_2}\right]^{1/2} \quad \ldots (17)$$

$$\mu_e = \frac{s_3 + s_2}{2}\left[\frac{hca^3}{2s_2}\right]^{1/2} \quad \ldots (18)$$

And

$$\mu_e = \left[\frac{s_3 + s_2}{s_3 - s_2}\right]\mu_g for(s_3 > s_2) \quad \ldots (19)$$

These different solvent polarity functions like Δf, f_1, f_2 *and* E_T^N whose values are obtained from literature [26-28] are used to calculate ground state and excited state dipole moments. Figure 8, Fig. 9 and Fig. 10 represent plot of Stokes' shift ($\overline{\Delta\nu}$) versus Δf, Stokes' shift ($\overline{\Delta\nu}$) versus f_1, and $\frac{1}{2}(\bar{\nu}_a + \bar{\nu}_f)$ versus f_2, respectively. The linear progression is done and the data is fit to a straight line, corresponding values of the slopes and correlations are mentioned in the respective graphs. All the graphs are made for number of data points n=5. The radius of the solute molecule is calculated from the molecular volume of molecule[24]. μ_g and μ_e are calculated from the slopes of respective plots using Eqs (17), (18) and (19) and are given in Table 3.

These equations do not consider the polarizability, hydrogen bonding effect and complex formation. For understanding polarization dependence of hydrogen bonding effect on spectral characteristics, normalized value called E_T^N is employed which includes both solvent polarity and protic hydrogen bond effect. The theoretical basis for the correlation as the spectral shift with E_T^N was proposed by Reichardt and given as:

$$\overline{\Delta\nu} = \bar{\nu}_a - \bar{\nu}_f = 11307.6\left[\left(\frac{\Delta\mu}{\Delta\mu_B}\right)^2\left(\frac{a_B}{a}\right)^3\right]E_T^N + constant \quad \ldots (20)$$

Where $\Delta\mu_B$ represents the change in dipole moment on excitation and a_B is Onsager cavity radius of

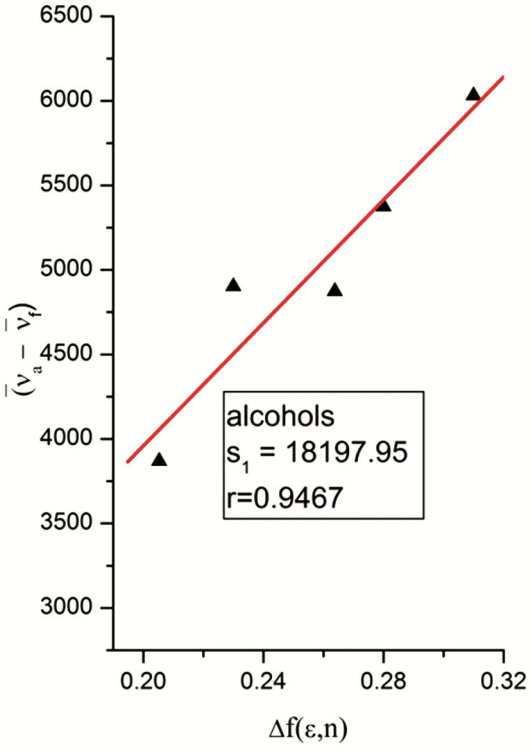

Fig. 8 – Plot of Stokes' shift ($\overline{\nu_a} - \overline{\upsilon_f}$) versus $\Delta f(\varepsilon,n)$ along with correlation co-efficient (r), slope (s_1) and number of data (n).

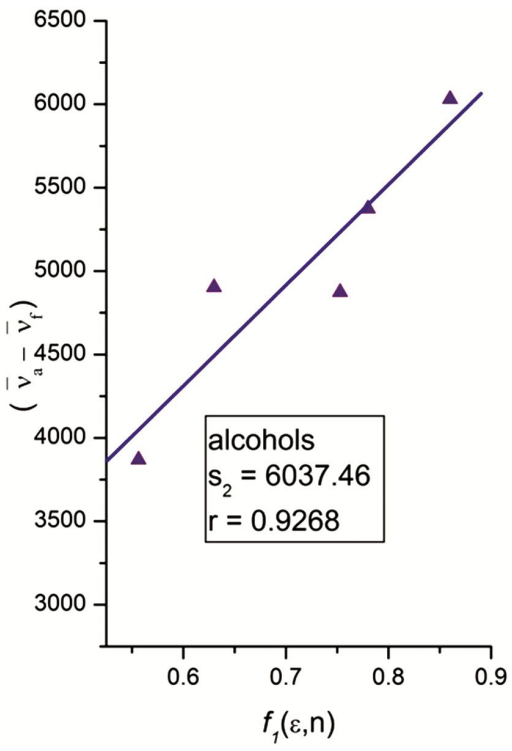

Fig. 9 – Plot of Stokes' shift ($\overline{\nu_a} - \overline{\upsilon_f}$) versus $f_1(\varepsilon,n)$ along with correlation co-efficient (r), slope (s_2) and no. of data (n).

betadine dye molecule.$\Delta\mu$ and a are the corresponding quantities for 2MPBA. $\Delta\mu$ can be evaluated from the slope (m) of the plot of Stoke's shift $\overline{\Delta\nu}$ versus E_T^N and is given by:

$$\Delta\mu = (\mu_e - \mu_g) = \sqrt{\frac{m \times 81}{(6.2/a)^3 \, 11307.6}} \quad \ldots (21)$$

A linear plot of stokes' shift with E_T^N with good correlation (shown in Fig. 11) encouraged us to calculate the excited state dipole moment using Eq. (21) and is given in Table 3. It is observed that the excited state dipole moments are greater than ground state dipole moments. The increase in the dipole moment is about 8.28 D in the excited state. This along with increased excited dipole moment by plot of E_T^N gives the evidence about the intra-molecular charge transfer (ICT) character in the emitting singlet state of the solute and the formation of inter-molecular hydrogen bonding[29]. The mismatch between this value and that obtained from Eq. (17) is attributed to the fact that, in the quantum chemical calculations molecules are assumed to be involved in the gas phase and does not include solvent interactions[30].

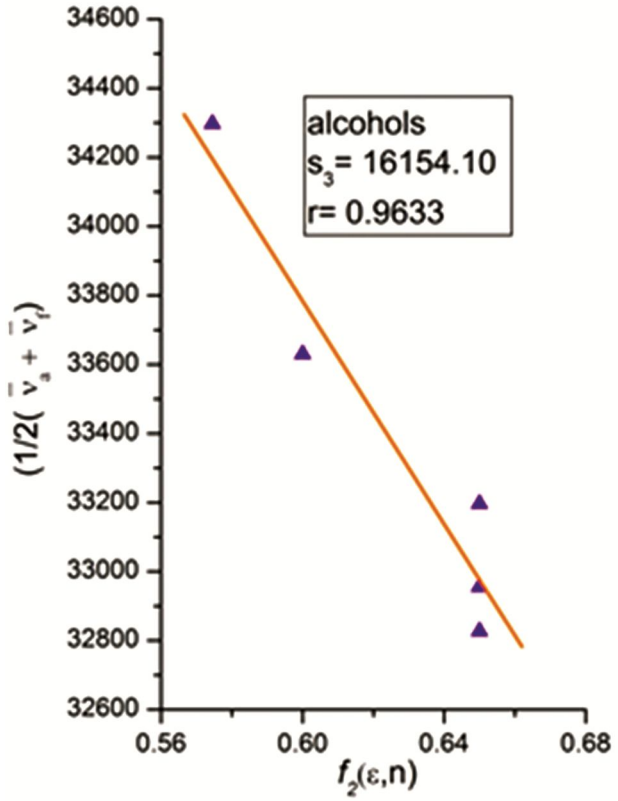

Fig. 10 – Plot of $1/2(\bar{\nu}_a + \bar{\nu}_f)$ versus f_2 (ε,n) along with correlation co-efficient (r), slope (s_3).

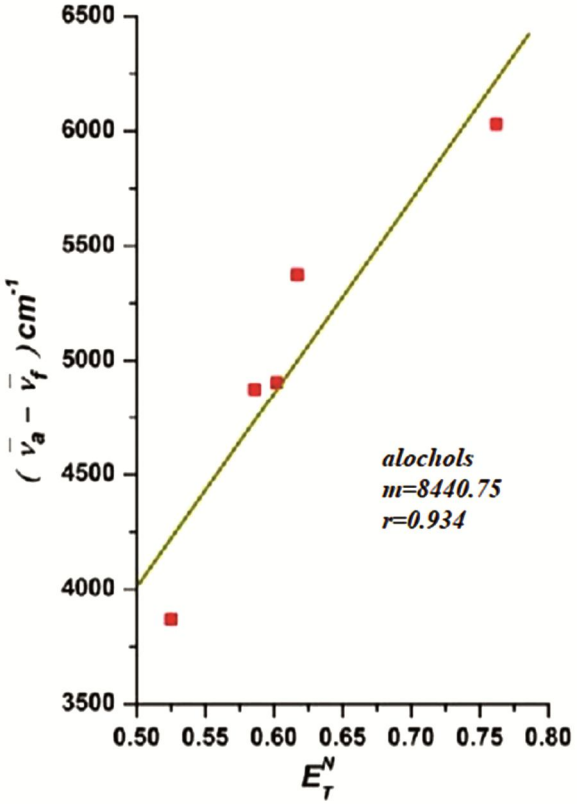

Fig. 11 – Plot of Stokes' shift as a function of E_T^N.

Table 3 – Radius of the molecule (a), calculated values of ground state (μ_g) and excited state (μ_e) dipole moments and change in the dipole moments($\Delta\mu$) in alcohols.

Solute	Radius (Å)	μ_g[a] (D)	μ_g[b] (D)	μ_e[c] (D)	μ_e[d] (D)	μ_e[e] (D)	μ_e[f] (D)	$\Delta\mu$[g]	$\Delta\mu$[h]
2MPBA	3.3613	2.5990	3.9970	8.7693	12.2810	8.7685	7.1009	8.2840	3.1039

D=Debye=3.33564×10^{-30} cm=10^{-18}esu cm

[a]Ground state dipole moment calculated using B3LYP functional with 6–31 g* basis using DFT.
[b] Experimental ground state dipole moments calculated from Eq. (17)
[c] Experimental excited-state dipole moments calculated from Eq. (18)
[d] Excited state dipole moments calculated from Lippert's Eq. (14)
[e] Excited state dipole moments calculated from Bakshiev's Eq. (15)
[f] Excited state dipole moments calculated from E_T^N parameter Eq. (21)
[g] Change in dipole moments for experimental μ_e[d] and μ_g[b]
[h] Change in dipole moments calculated from E_T^N parameter Eq. (21)

4 Conclusions

The gradual decrease in the fluorescence intensity with increase in [*Q*] confirms the effective quenching of fluorophores by aniline. The negative deviation in the *S-V* plots suggests the existence of two or more emitting species in the studied molecule. The negative deviation in the *S-V* plots is attributed to the conformational changes that arise from the formation of intramolecular and intermolecular hydrogen bonds between solutes and alcohols.

Spectroscopic investigations of dipole moments of the boronic leads to conclude that the ground state of the solute is moderately affected by the solvent polarity whereas the solvent polarity has greater effect on the excited states. Stokes' shift is an indication of $\pi \rightarrow \pi^*$ transitions that are taking place in the excited states. The role of intra-molecular charge transfer (ICT) character in the emitting singlet state is confirmed by increase in the excited state dipole moments.

Acknowledgement

The author (RMM) is grateful to Dr N V R Naidu Principal, RIT, Dr A Jagannath Reddy, HOD, Department of Physics, RIT and the management of RIT, Bangalore for their encouragement and providing necessary requirements.

References

1 Dennis G H, *Applications of boronic acids in chemical biology and medicinal chemistry*, (Wiley Online Library), 2011.
2 Cao Z, Nandhikonda P & Heagy M D, *J Org Chem*, 74 (2009) 3544.
3 Lorand J P & Edwards J O, *J Org Chem*, 24 (1959) 69.
4 Springsteen G & Wang B, *Tetrahedron*, 585 (2002) 291.
5 Wang W, Gao X & Wang B, *Curr Org Chem*, 6 (2002) 1285.
6 Strawbridge S M, Green S J & Tucker J H R, *Chem Commun*, 2000 (2000) 2393.
7 Gary A M, Trice S L J & Dreher S D, *J Am Chem Soc*, 132 (2010) 17701.
8 Nagaraja D, Melavanki R M & Patil N R, *Can J Phys*, 91(2013) 966.
9 Elfeky S A, Flower S E, Masumoto N, D'Hooge F, Labarthe L, Chen W, Len C, James T D & Fossey J S, *Chem Asian J*, 5 (2010) 581.
10 Lackowicz J R, *Principles of fluorescence spectroscopy*, (Plenum Press: New York), 1999.
11 Melavanki R M, Kusanur R A, Kulakarni M V & Kadadevarmath J S, *J Luminescence*, 128 (2007) 573.
12 Behra P K, Mukherjee T & Mishra A K, *J Luminescence*, 65 (1995) 131.
13 Nagaraja D, Melavanki R M, Patil N R & Kusanur R A, *Spectrochim Acta Part A*,130 (2014) 122.
14 Geethanjali H S, Nagaraja D & Melavanki R M, *J Mol Liq*, 209 (2015) 669.
15 Geethanjali H S, Nagaraja D, Melavanki R M & Kusanur R A, *J Luminescence*, 167 (2015) 216.
16 Andre J C, Niclause M & Ware W R, *Chem Phys*, 28 (1978) 371.
17 Valeur B, *Molecular fluorescence: Principles and application*, (Wiley-VCH: Weinheim), 2002.
18 Rohatgi-Mukherjee K K, *Fundamental of photochemistry*, (Wiley Eastern Ltd), 1992.
19 Hunt T, *J Fluoresc*, 14 (2004) 217.
20 Naik A B, Naik L R, Kadadevarmath J S, Pal H & Rao V J, *J Photochem Photobiol* A: 214 (2010) 145.
21 Samworth C M, Esposti M D & Lenaz G, *Eur J Biochem*, 171 (1988) 81.
22 Leherer S S, *Biochemistry*, 10 (1971) 3254.
23 Webber S E, *J Photochem Photobiol*, 65 (1997) 33.
24 Molinspiration Cheminformatics. Monolinperation. 2017. Available from http://wwwmolinspirationcom/cgi-bin/properties.
25 Einstein A, *Investigations on the theory of brownian movement*, (Dover: New York), 1956.
26 Melavanki R M, Patil H D, Umapathy S & Kadadevaramath J S, *J Fluoresc*, 22 (2012) 137.
27 Melavanki R M, Patil N R, Kapatkar S B, Ayachit N H, Siva U, Thipperudrappa J & Nataraju A R, *J Mol liq*, 158 (2011) 105.
28 Patil N R, Melavanki R M, Kapatkar S B, Ayachit N H & Saravanan J, *J Fluoresc*, 21 (2011) 1213.
29 Pang Y H, Shung S M, Wong M S, Li Z H & Dong C, *J Photochem Photobiol A: Chem*, 170 (2005) 15.
30 Acemioglu B, Arik M & Efeoglu H, *Mol Struc (Theochem*), 548 (2001) 165.